DOI: 10.1002/ejic.200500681

# Structural Studies of Keggin-Type Polyoxotungstates by Extended X-ray Absorption Fine Structure Spectroscopy

**M. Salete S. Balula,[a] Isabel C. M. S. Santos,[a] José A. F. Gamelas,[a] Ana M. V. Cavaleiro,*[a] Norman Binsted,[b] and Walkiria Schlindwein[c]**

**Keywords:** Polyoxometalates / Keggin / EXAFS spectroscopy

Extended X-ray absorption fine structure spectroscopy (EXAFS) was used to characterize several Keggin-type polyoxotungstates (tetrabutylammonium salts) in the solid state and in acetonitrile solution. The polyoxometalates studied were $[PW_{12}O_{40}]^{3-}$ (the parent Keggin anion), $[PW_{11}O_{39}]^{7-}$ (a lacunary anion), $[PW_{11}M(H_2O)O_{39}]^{4-}$, M = Fe, Ru, and $[XW_{11}Mn^{III}(H_2O)O_{39}]^{n-}$, X = P, Si, B (transition-metal-substituted anions). The role of multiple-scattering contributions was evaluated for $[PW_{12}O_{40}]^{3-}$ for which an accurate structure determination was available. The results from the multiple-scattering analyses were compared with the single-scattering method. The average W-shell inter-atomic distances were determined in relation to a selected tungsten atom ($W_c$) by W $L_{III}$ edge transmission analysis. Several shells of up to 3.8–4.0 Å were identified. For the anion $[PW_{12}O_{40}]^{3-}$, the obtained inter-atomic distances in the solid sample and in acetonitrile were identical but for the lacunary anion the EXAFS spectrum of the solid was different from that in solution (the number of atoms coordinated to $W_c$ in $[PW_{11}O_{39}]^{7-}$ was the same in both cases, but the calculated distances for the shells were slightly different). Metal-substituted anions were studied by W $L_{III}$ edge transmission and by Fe, Mn, or Ru *K* edge fluorescence analysis. The average coordination sphere of tungsten was affected by the replacement of a W=O by a M–$OH_2$ group. The EXAFS results indicate that on average the $MnO_6$ octahedron is larger than $FeO_6$ or $RuO_6$ and also larger than the average of all $WO_6$ octahedra in $[PW_{11}M(H_2O)O_{39}]^{4-}$. This was attributed to the occurrence of the Jahn–Teller effect in the coordination sphere of $Mn^{III}$. A comparison of the W $L_{III}$ edge analysis EXAFS data for three $Mn^{III}$-substituted anions (X = P, Si, B) suggested that the average size of the $W_3O_{13}$ groups did not depend on X.


## Introduction

Keggin-type polyoxometalates[1–4] have been continuously studied in the last decade due to their interesting properties and possible applications in various fields, like catalysis,[5,6] materials science,[7] and medicine.[8] The Keggin-type polyoxotungstates include a large number of anions structurally related to the parent Keggin anions, α-$[XW_{12}O_{40}]^{n-}$, X = P, Si, B, etc., namely the lacunary, α-$[XW_{11}O_{39}]^{n-}$, and the metal-monosubstituted polyoxotungstates, α-$[XW_{11}M(H_2O)O_{39}]^{n-}$, M = transition or p-block metal, among others.[1,9]

The structure of the α isomer of $[PW_{12}O_{40}]^{3-}$ ($PW_{12}$) has been known since 1933[10] and is presented in Figure 1 (a). The twelve $WO_6$ octahedra, arranged in four corner shared $W_3O_{13}$ groups, surround a central tetrahedral $PO_4$ group, forming a tungsten–oxygen cluster with overall $T_d$ symmetry. Each $W_3O_{13}$ group comprises three edge-sharing $WO_6$ octahedra. This structure was found for a variety of other $[XMo_{12}O_{40}]^{n-}$ and $[XW_{12}O_{40}]^{n-}$ anions.[1] Only the α-isomers will be considered in this paper and the prefix will be omitted hereafter.

Only a few crystallographic studies are known for simple salts of the lacunary and monosubstituted Keggin-type polyoxotungstates.[1,9] The disorder observed for the $XO_4$ central group and also for the substituting $MO_6$ group (over twelve positions) usually precludes the determination of the structures with acceptable refinement parameters and no information can be given for the structural environment around M. Exceptions were found for a few compounds, namely $[Et_3NH]_5[XW_{11}Co^{II}O_{39}]\cdot 3H_2O$ (X = P, As),[11] $(ET)_8[PW_{11}Mn^{II}O_{39}]\cdot 2H_2O$,[12,13] and $(ET)_8[PW_{11}Ni^{II}(H_2O)O_{39}]\cdot 2H_2O$,[13] in which the metals M were disordered over two positions, $[Co(dpa)_2(H_2O)_2]_2[Hdpa][PW_{11}Co^{II}O_{39}]$,[14] $(Hpbpy)_5[PW_{11}Co^{II}(pbpy)O_{39}]\cdot 2H_2O$,[15] and $[Ni(DETA)_2]_3[SiW_{11}Ni^{II}O_{39}]\cdot 2.5H_2O$[16] [ET = bis(ethylenedithio)tetrathiafulvalene, dpa = di(2-pyridyl)amine, pbpy = 5-phenyl-2-(4-pyridinyl)pyridine, DETA = diethylenetriamine]. The formation of chains of linked heteropolyanions was observed for most of these compounds.

[a] Department of Chemistry, University of Aveiro, 3810-193 Aveiro, Portugal
Fax: +351-234-370084
E-mail: ana@dq.ua.pt
[b] CCLRC Daresbury Laboratory, Warrington, WA4 4AD, UK
[c] Leicester School of Pharmacy, De Montfort University, LE1 9BH, Leicester, UK

  

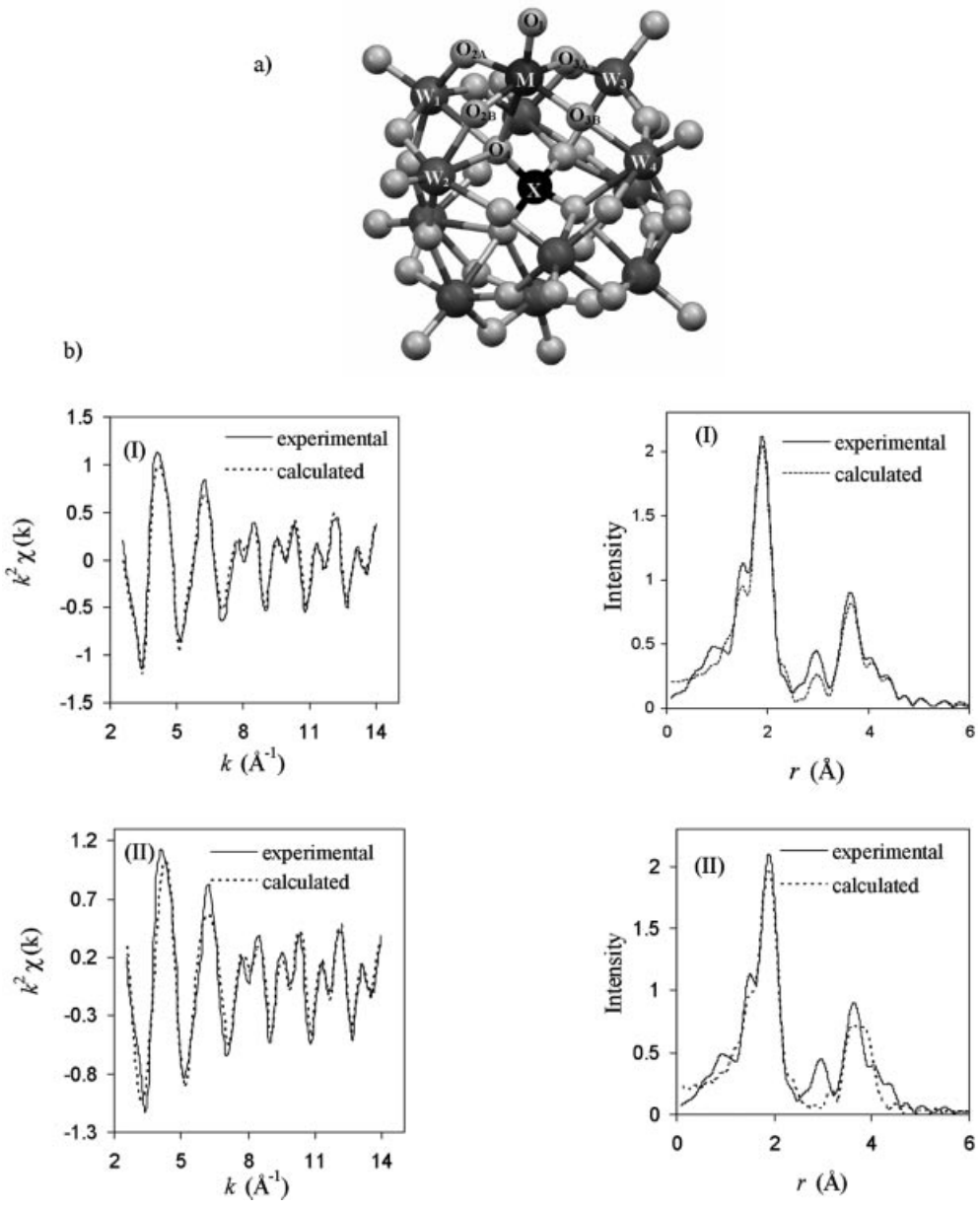


Figure 1. (a) The structure of the Keggin-type polyoxoanions (M = W, Fe, Mn, Ru). (b) EXAFS fit to $k^2\chi(k)$, and Fourier transform of $[PW_{12}O_{40}]^{3-}$: (I) multiple scattering calculation using crystallographic coordinates[25] with refined Debye–Waller factors, $E_f$ and AFAC; (II) using refined shell parameters.

An approach to the solution of the problem created by the disorder of X-ray crystal structures can be given by the use of extended X-ray absorption fine structure (EXAFS) spectroscopy. Information regarding the coordination sphere of W, the substituting metal M (first shell), and other longer-distance interactions (farther shells), up to about 4 Å, is, in many cases, possible. Besides, the EXAFS technique has the advantage that the measurements can be made in solids as well as in solution. Polyoxometalates have already been studied by EXAFS and related techniques. Particularly, studies on Keggin-type heteropolyanions, the majority performed in the solid state, have been published. Evans et al. used EXAFS to characterize the structure of $[PMo_{12}O_{40}]^{3-}$ and $[PW_{12}O_{40}]^{3-}$.[17] Previous studies in this area have been performed by Watanabe and coworkers.[18] Zhang and Pope investigated the nature of the ligand (L) coordinated to the Mn atom within the $[ZnW_{11}Mn^{IV}(L)O_{39}]^{6-}$ and $[ZnW_{11}Mn^{II}(L)O_{39}]^{8-}$ heteropolyanions.[19] EXAFS was used to determine the local structure of tetrahedral $Co^{III}$ in $[CoW_{12}O_{40}]^{5-}$.[20] Other published studies concerned supported $[PW_{12}O_{40}]^{3-}$ (mainly to confirm the presence of the anion) and vanadium-substituted tungstophosphates.[21] Studies of Keggin polyoxomolybdates that are related to their use in heterogeneous catalysis (e.g. formation of the anions on supports, thermal stability, environment of substituting metals) are also found.[22,23] Studies

  

referring to non-Keggin heteropolyanions were also reported.[24] In general, it can be summarized that EXAFS and related techniques were used to probe the coordination geometry or oxidation states of different metals encapsulated, coordinated, or supported by the polyoxometalates and the formation or stability of the heteropolyanions (mostly heteropolymolybdates) on heterogeneous catalysts. In spite of the importance of Keggin-type anions in homogeneous oxidative catalysis,[5] no studies in solution in conditions used in homogeneous catalysts have been reported so far.

In this work, EXAFS results are reported regarding the structural aspects of W and M in the tetrabutylammonium (TBA) salts of the Keggin-type anions $[PW_{11}O_{39}]^{7-}$ ($PW_{11}$), $[PW_{11}M(H_2O)O_{39}]^{4-}$ ($PW_{11}M$), M = Fe, Ru, and $[XW_{11}Mn^{III}(H_2O)O_{39}]^{n-}$ ($XW_{11}M$), X = P, Si, B. The role of multiple scattering contribution was evaluated for $[PW_{12}O_{40}]^{3-}$ ($PW_{12}$) for which an accurate structure was available that was determined by neutron diffraction.[25] The average inter-atomic distances in the series of anions formed when one tungsten atom of dodecatungstophosphate is removed to create a vacancy or is substituted isomorphically by a transition metal, $M^{III}$ = Fe, Mn, and Ru, are compared in the solid state and in acetonitrile solution. Structural data for the majority of these compounds are given for the first time. Some of these salts have been found to be good catalysts for the oxidation of cycloalkanes and other organic comounds with hydrogen peroxide in acetonitrile[26–28] and this prompted us to use this solvent in our studies with the aim of obtaining results that may be used in future studies on the stability of Keggin anions in homogeneous catalytic conditions.

## Results and Discussion

### The Keggin Heteropolyanion, $[PW_{12}O_{40}]^{3-}$ – Multiple versus Single Scattering Analysis

Multiple scattering (MS) generally makes a significant contribution to XAFS.[29] At low energy covalent clusters may give a massive contribution to the "white line", associated with resonant scattering of a photoelectron. The significance of these paths is such that unless the near edge region is entirely avoided the effect will be seen even in the Fourier transform of the first shell. At higher energies the paths will certainly make large contributions where the forward scattering path angles are 150° or more. Other paths may or may not give significant effects. Quite often, the main effect is a phase change over all or part of the spectrum, which may be especially conspicuous near a scattering minimum associated with an $l > 1$ final state. However, these are only general rules and for any specific structure it is necessary to compare results with and without multiple scattering before presuming to adopt the single-scattering approximation.

The role of MS was evaluated for $[PW_{12}O_{40}]^{3-}$, for which an accurate structure was available determined by neutron diffraction.[25] This allowed the EXAFS data to be fitted with no adjustable parameters other than a small number of Debye–Waller terms (for groups of shells of similar type and distance), the energy zero $E_f$, and the overall amplitude AFAC. The result, using a cluster of 6 Å radius, with 3796 MS paths to the fifth order, is shown in Figure 1 (b, I). The *R* factor obtained was 19%, which is considered good given that no structural variables were involved. Most of the error actually appears to be involved in residual low-frequency background contributions rather than any intrinsic inaccuracy in the technique. Multiple scattering makes an important contribution, but this is dominated by a small number of paths: principally the W–O–W second and third order paths with bond angles close to 120 or 150°. The number of structural parameters required to describe this cubic phase is small, but this is not the case for the lacunary or monosubstituted compounds, for which published structures show a low symmetry with several different metal sites, and oxygen polyhedra of $C_1$ or $C_2$ symmetry. For these, a simplified model is required using a reduced number of shells and without multiple scattering, which requires the addition of more parameters to describe the bond angles. To test the validity of this we repeated the analysis using only seven shells, and without multiple scattering. The fit, shown in Figure 1(b, II), gave an *R* factor of 26%, which is considered acceptable, and although the distances are different they differ by no more than 0.03 Å. The results are shown in Table 1. Given that this is only an approximate structural model, errors of this magnitude can be expected, and we believe that the results obtained are sufficient to draw the conclusions we do concerning the nature of the oxygen octahedra and metal–metal distances in the cluster. This approach was therefore used throughout this paper.

Table 1. Theoretical EXAFS best-fit parameters for $[PW_{12}O_{40}]^{3-}$ with and without multiple scattering. Data obtained from neutron diffraction.[25] $E_f$ is the edge position relative to the photoelectron wavevector (eV); $R_x$ refer to the distances (in angstroms) and *A* are the Debye–Waller Factor terms (in Å$^2$); the *R* factor gives a meaningful indication of the quality of the fit in *k* space (in%).

| | Multiple scattering (3796 paths) | Simplified single scattering |
|---|---|---|
| Shells | **33** | **7** |
| R1 (1 × O) | 1.715 | 1.737 (0.019) |
| R2 (2 × O) | 1.915 | 1.919 (0.007) |
| R3 (2 × O) | 1.921 | 1.919 |
| R4 (1 × O) | 2.445 | 2.459 (0.039) |
| R5 (2 × W) | 3.435 | 3.446 (0.019) |
| R6 (1 × O) | 3.574 | |
| R7 (1 × P) | 3.578 | 3.557 (0.061) |
| R8 (1 × O) | 3.645 | |
| R9 (2 × W) | 3.720 | 3.748 (0.016) |
| *A*[1] | 0.004 (0.002) | 0.004 |
| *A*[2–3] | 0.005 (0.001) | 0.004 (0.001) |
| *A*[4] | 0.014 (0.001) | 0.009 (0.011) |
| *A*[6,8] | 0.017 (0.013) | |
| *A*[7] | 0.004 (0.008) | 0.004 (0.008) |
| *A*[5,9] | 0.004 (0.001) | 0.005 (0.002) |
| $E_f$ (eV) | –11.6 | –12.3 |
| *R* (%) | 19.0 | 26.4 |

  

Data were collected for solid $TBA_3[PW_{12}O_{40}]$ as well as in acetonitrile solution. The fitted results of the EXAFS experimental data are presented in Table 2. The average W-shell inter-atomic distances are determined in relation to a selected tungsten atom referred here as $W_c$. Results for the solid sample are in good agreement with those of the previous EXAFS study by Evans et al.[17] and with the reported diffraction data.[25] They are presented here for comparison with results obtained for $[PW_{12}O_{40}]^{3-}$ in solution and for the other Keggin-type anions. From the results in Table 2 it can be seen that the structure of the $[PW_{12}O_{40}]^{3-}$ anion does not change when the compound is dissolved in acetonitrile. The differences in bond lengths and Debye–Waller factors for the shells fitted in both cases (solid and in acetonitrile solution) are within the standard deviation. These results parallel those observed previously for the related $[PMo_{12}O_{40}]^{3-}$ anion.[17]

Table 2. Experimental EXAFS best-fit parameters for the Keggin heteropolyanion in $TBA_3[PW_{12}O_{40}]$ (W $L_{III}$ edge transmission mode). Parameters as defined in Table 1.

| Shells | Solid state | $CH_3CN$ solution | Published data EXAFS[17] | Neutron diffraction[25] |
|---|---|---|---|---|
| R1 (1×O) | 1.697 (0.006) | 1.697 (0.008) | 1.710 | 1.715 |
| R2 (2×O) | 1.915 (0.002) | 1.917 (0.006) | 1.898 | 1.915 |
| R3 (2×O) | 1.915 (0.002) | 1.917 (0.006) | 1.898 | 1.921 |
| R4 (1×O) | 2.304 (0.017) | 2.318 (0.027) | | 2.445 |
| R5 (2×W) | 3.459 (0.008) | 3.461 (0.012) | 3.403 | 3.435 |
| R6 (1×O) | | | | 3.574 |
| R7 (1×P) | 3.545 (0.015) | 3.540 (0.020) | | 3.578 |
| R8 (1×O) | | | | 3.645 |
| R9 (2×W) | 3.733 (0.014) | 3.736 (0.013) | 3.680 | 3.720 |
| *A*[1] | 0.005 (0.001) | 0.004 (0.002) | 0.009 | |
| *A*[2–3] | 0.009 (0.001) | 0.010 (0.001) | 0.012 | |
| *A*[4] | 0.016 (0.006) | 0.017 (0.001) | | |
| *A*[7] | 0.005 (0.001) | 0.005 (0.002) | | |
| *A*[5,9] | 0.010 (0.002) | 0.010 (0.003) | 0.011 | |
| $E_f$ (eV) | –11.4 | –14.0 | | |
| *R* (%) | 20.8 | 30.5 | | |

In agreement with the known Keggin structure, six oxygen atoms were found around $W_c$ (only five had been detected by Evans et al.[17]). For the solid sample, the shortest observed bond length between tungsten and oxygen, attributed to the terminal oxygen atoms ($O_1$, Figure 1, a, M = $W_c$), was 1.697 Å. Four bridging oxygen atoms ($O_{2a}$, $O_{2b}$, $O_{3a}$, $O_{3b}$) were found at a distance of 1.915 Å from $W_c$ and the oxygen of the central $PO_4$ tetrahedron ($O_4$) at a distance of 2.304 Å. Each oxygen atom from the central $PO_4$ tetrahedron belongs to one of the four $W_3O_{13}$ groups. Two tungsten atoms at a distance of 3.459 Å probably belong to the same $W_3O_{13}$ group as $W_c$ ($W_1$ and $W_2$, Figure 1, a), whereas two tungsten atoms at a distance of 3.733 Å must be located in different $W_3O_{13}$ groups in relation to $W_c$ ($W_3$ and $W_4$, Figure 1, a). The distance between $W_c$ and the phosphorus atom of the central $PO_4$ tetrahedron is 3.545 Å. The inclusion of one phosphorus atom improved the *R* value; however, the improvement was even more significant when tungsten atoms were introduced at 3.733 Å. The results obtained for the dodecatungstophosphate in the solid state and in acetonitrile solution (Table 2) are very similar.

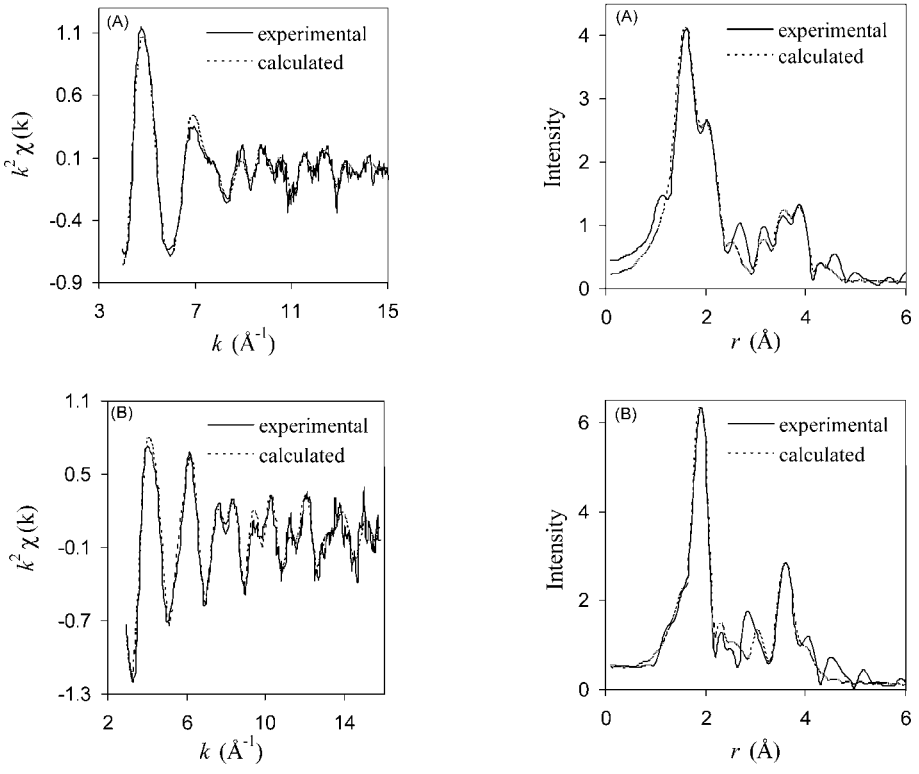


Figure 2. W $L_{III}$ edge EXAFS spectrum and Fourier transform for the $[PW_{11}O_{39}]^{7-}$ anion in $TBA_4H_3[PW_{11}O_{39}]$: (a) solid state; (b) $CH_3CN$ solution.

  

### The Lacunary Polyoxoanion, $[PW_{11}O_{39}]^{7-}$

The lacunary anion $[PW_{11}O_{39}]^{7-}$ has a Keggin structure from which one W=O group was removed. In this case not all W atoms are equivalent because four of the eleven W atoms have two terminal oxygen atoms. Figure 2 shows the EXAFS spectrum and the Fourier transform for the $PW_{11}$ anion. In this case the spectrum of the solid was different from that obtained in solution. The fit of the EXAFS results is presented in Table 3. The average number of atoms coordinated to $W_c$ (average of all tungsten atoms presented in the structure) was the same in both cases, but the calculated distances for the shells are slightly different. The structure of the lacunary anion is globally less rigid than that of the parent $PW_{12}$. This may be the reason that different distance values were observed for the anion in the solid state and in $CH_3CN$ solution, reflecting different environments in each case, contrary to what was observed for $PW_{12}$.

Table 3. EXAFS best-fit parameters for the lacunary heteropolyanion in $TBA_4H_3[PW_{11}O_{39}]$ (W $L_{III}$ edge transmission mode). Parameters as defined in Table 1.

| Shells | Solid state | $CH_3CN$ solution |
|---|---|---|
| R1 (1 × O) | 1.641 (0.004) | 1.782 (0.014) |
| R2 (2 × O) | 1.761 (0.005) | 1.937 (0.003) |
| R3 (2 × O) | 2.205 (0.007) | 2.121 (0.017) |
| R4 (1 × O) | 2.412 (0.022) | 2.436 (0.012) |
| R5 (2 × W) | 3.394 (0.009) | 3.457 (0.005) |
| R7 (1 × P) | 3.346 (0.028) | 3.220 (0.012) |
| R9 (2 × W) | 3.919 (0.029) | 3.765 (0.016) |
| *A*[1] | 0.008 (0.001) | 0.019 (0.004) |
| *A*[2–3] | 0.015 (0.002) | 0.010 (0.002) |
| *A*[4] | 0.015 (0.005) | 0.004 (0.002) |
| *A*[7] | 0.023 (0.008) | 0.005 (0.002) |
| *A*[5,9] | 0.023 (0.007) | 0.012 (0.004) |
| $E_f$ (eV) | 10.2 | 13.5 |
| *R* (%) | 22.5 | 21.8 |

From the EXAFS fit of the lacunary anion four shells of oxygen atoms were deduced in the first coordination sphere of $W_c$. In the solid state the shortest oxygen–tungsten bond length was 1.641 Å and corresponds to the average of the W–O distance to the oxygen atoms protruding from the anion. The value of 1.761 Å is possibly the average of terminal (oxygen atoms surrounding the lacuna) and bridging W–O bond lengths. This is a consequence of the fact that each of the W atoms surrounding the lacuna is bound to two monocoordinated oxygen atoms. Other bridging oxygen atoms are located at a distance of 2.205 Å. Finally, the W–O distance to the oxygen of the central $PO_4$ group was found to be 2.412 Å. These values are comparable to those reported for $[PW_{11}O_{39}]^{7-}$[30] and $[SiW_{11}O_{39}]^{8-}$,[31] obtained by X-ray crystallography. In these studies the position of the vacancy could not be located with certainty.[30,31]

### W $L_{III}$ Edge Analysis of Monosubstituted Polyoxoanions, $[PW_{11}M(H_2O)O_{39}]^{4-}$, M = Fe and Mn

It is commonly accepted that the Keggin structure is maintained when one W=O group from the anion $[PW_{12}O_{40}]^{3-}$ is substituted by $M^{III}–OH_2$, M = transition metal, to form $[PW_{11}M(H_2O)O_{39}]^{4-}$ and the results here presented for M = Fe, Mn are in agreement with this fact. Figure 3 shows the W $L_{III}$ edge EXAFS spectrum and the Fourier transform for the solid samples of TBA salts of $PW_{11}Mn$ and $PW_{11}Fe$. The results from the curve fitting are presented in Table 4. For these anions, the EXAFS data obtained from the W $L_{III}$ edge analysis are the average of the eleven tungsten atoms in an octahedral coordination.

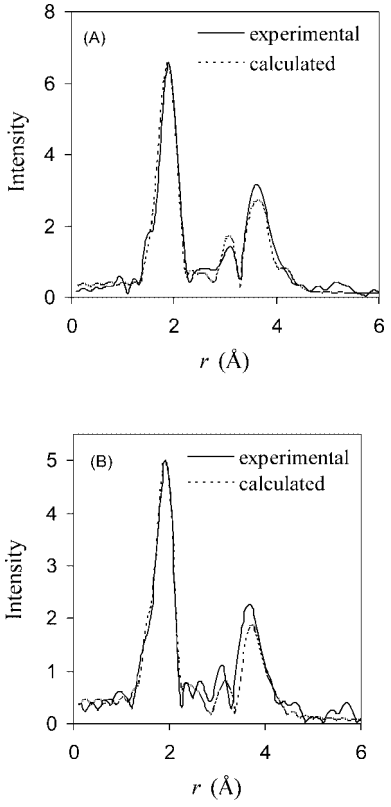


Figure 3. W $L_{III}$ edge Fourier transform for $[PW_{11}Fe(H_2O)O_{39}]^{4-}$ (a) and $[PW_{11}Mn(H_2O)O_{39}]^{4-}$ (b) in solid state TBA salts.

Table 4. EXAFS best-fit parameters for solid $TBA_4[PW_{11}Fe^{III}(H_2O)O_{39}]\cdot H_2O$ and $TBA_4[PW_{11}Mn^{III}(H_2O)O_{39}]$ (W $L_{III}$ edge transmission mode). Parameters as defined in Table 1.

| Shells | $PW_{11}Fe$ solid state | Shells | $PW_{11}Mn$ solid state |
|---|---|---|---|
| R1 (1 × O) | 1.628 (0.014) | R1 (2 × O) | 1.705 (0.016) |
| R2 (3 × O) | 1.944 (0.003) | R2 (2 × O) | 1.931 (0.007) |
| R3 (2 × O) | 2.131 (0.015) | R3 (2 × O) | 2.225 (0.028) |
| $R_{Fe}$ (1 × Fe) | 2.994 (0.016) | $R_{Mn}$ (1 × Mn) | 2.564 (0.040) |
| R5 (1 × W) | 3.234 (0.013) | R5 (1 × W) | 3.034 (0.031) |
| R7 (1 × P) | 3.583 (0.032) | R7 (1 × P) | 4.168 (0.061) |
| R9 (2 × W) | 3.767 (0.011) | R9 (2 × W) | 3.730 (0.035) |
| *A*[1] | 0.029 (0.004) | *A*[1] | 0.020 (0.005) |
| *A*[2–3] | 0.010 (0.002) | *A*[2–3] | 0.010 (0.002) |
| *A*[Fe] | 0.016 (0.004) | *A*[Mn] | 0.034 (0.005) |
| *A*[7] | 0.005 (0.004) | *A*[7] | 0.010 (0.006) |
| *A*[5,9] | 0.011 (0.002) | *A*[5,9] | 0.016 (0.004) |
| $E_f$ (eV) | 10.9 | $E_f$ (eV) | 12.1 |
| *R* (%) | 26.5 | *R* (%) | 29.9 |

  

As found for $PW_{12}$ and $PW_{11}$, the $W_c$ atom of $PW_{11}Fe$ has six oxygen atoms in the first coordination sphere with bond lengths of 1.628 Å, 1.944 Å, and 2.131 Å (Table 4). These average distances do not differ much from those of the $PW_{12}$ unit. The Fe atom was located at a distance of 2.994 Å from $W_c$ and the nearest W atom at a distance of 3.234 Å. These distances are close enough to suggest that the W is localized within a $W_cWFeO_{13}$ group. The shortest W–$W_c$ distance obtained for $PW_{12}$ was 3.459 Å (Table 2). These values seem to indicate that when Fe replaces one W atom from a $W_cW_2O_{13}$ unit (in $PW_{12}$) it stays closer to $W_c$ than the replaced W was in the $PW_{12}$ structure. Also, the distance from $W_c$ to the four coordinated oxygen atoms of the $W_c$–O–P bridge is shorter in the iron anion than in $PW_{12}$. Therefore, even if the structure of the polyoxoanion is not globally altered the coordination sphere of tungsten is affected by the change of the W atom (with its terminal oxygen) for Fe, possibly with a terminal water molecule as a ligand.

For the $[PW_{11}Mn(H_2O)O_{39}]^{4-}$ polyoxoanion, the $W_c$–O bond lengths within the $W_cO_6$ octahedron (Table 4) were similar to the analogous bond lengths for $PW_{12}$. The terminal oxygen is at a distance of 1.705 Å from $W_c$, and the bridging oxygen atoms are at distances in the range of 1.931–2.225 Å. One tungsten atom from a $W_cWMnO_{13}$ group ($W_2$, 3.034 Å) and two other from a different $W_3O_{13}$ group ($W_3$ and $W_4$, 3.730 Å) are also at a close distance to the $W_c$ atom.

In the case of the $PW_{12}$ anion the four equatorial $W_c$–O(–W) bond lengths have the same value. This is not the case for $PW_{11}Fe$ and $PW_{11}Mn$, for which one of these distances was found to be longer than the other three, reflecting the loss of symmetry associated with the replacement of tungsten by a different transition metal.

The average of the W–O bond lengths around $W_c$ in $PW_{12}$, $PW_{11}Fe$, and $PW_{11}Mn$ are 1.94, 1.95, and 1.95 Å, respectively. However, the Mn seems to be closer (2.564 Å) to the $W_c$ atom than the Fe (2.994 Å) in the structure of $PW_{11}Fe$. These differences may be related to a higher distortion of the $W_cWMO_{13}$ group in the case of Mn, possibly as a consequence of the Jahn–Teller effect of the $Mn^{III}$ ion.

### Fe *K* Edge Analysis of $[PW_{11}Fe(H_2O)O_{39}]^{4-}$

Polyoxoanions like $PW_{11}Fe$ and $PW_{11}Mn$, with two different transition metals in their structure, have the advantage of providing two different elements for EXAFS studies. Curve-fitting results for the Fe *K* edge fluorescence EXAFS data for $PW_{11}Fe$ in the solid state and in $CH_3CN$ solution are presented in Figure 4 and Table 5. It was assumed for all M substituted anions that no replacement of the coordinated water of the M–$OH_2$ group by acetonitrile occurred. The results indicate that the structures around Fe are very similar in both media. On comparing the distances of the six oxygen atoms to Fe in the $FeO_6$ octahedron (values for the solid state and in solution are in the range 1.943–2.512 and 1.976–2.522 Å, respectively, Table 5) with those of the six oxygen–tungsten bonds in the $WO_6$ octahedra of the parent Keggin anion (1.697–2.318 Å, first three shells in

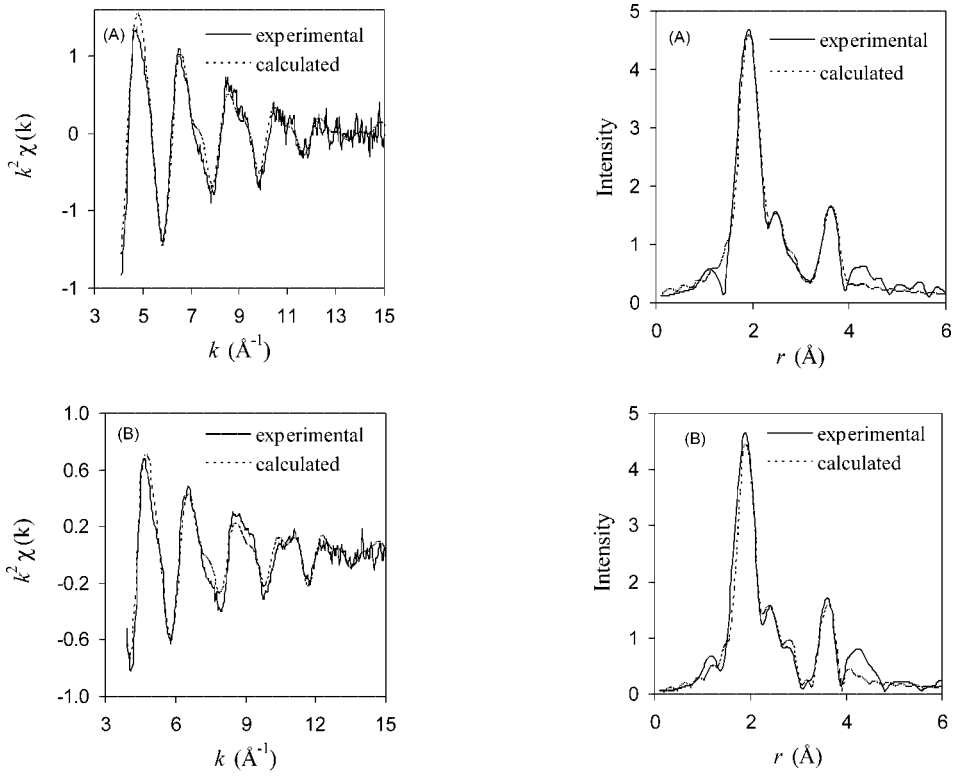


Figure 4. Fe *K* edge EXAFS spectrum and Fourier transform for $[PW_{11}Fe(H_2O)O_{39}]^{4-}$ in solid state TBA salt (a) and in $CH_3CN$ solution (b).

  

Table 2), it can be noticed that the $FeO_6$ octahedron is larger than the $WO_6$ that it has substituted. It is also larger than the nearest $WO_6$ octahedra (Table 4).

Table 5. EXAFS best-fit parameters for $TBA_4[PW_{11}Fe^{III}(H_2O)O_{39}]\cdot H_2O$ (Fe *K* edge fluorescence mode). Parameters as defined in Table 1.

| Shells | Solid state | $CH_3CN$ solution |
|---|---|---|
| R2 (2 × O) | 1.943 (0.040) | 1.976 (0.010) |
| R3 (2 × O) | 2.361 (0.031) | 2.390 (0.020) |
| R4 (2 × O) | 2.512 (0.025) | 2.522 (0.020) |
| R5 (2 × W) | 3.181 (0.045) | 3.247 (0.022) |
| R7 (1 × P) | 3.105 (0.041) | 3.156 (0.012) |
| R9 (2 × W) | 3.523 (0.097) | 3.547 (0.029) |
| *A*[2] | 0.010 (0.002) | 0.020 (0.005) |
| *A*[3] | 0.022 (0.008) | 0.026 (0.004) |
| *A*[4] | 0.010 (0.005) | 0.004 (0.002) |
| *A*[7] | 0.020 (0.010) | 0.016 (0.005) |
| *A*[5,9] | 0.018 (0.008) | 0.015 (0.004) |
| $E_f$ (eV) | 10.2 | 11.1 |
| *R* (%) | 30.0 | 30.1 |

Polyoxotungstophosphates with $Fe^{III}$ have been structurally characterized by Li et al.[32] and by Hill and collaborators.[33] The former determined the structure of the dimeric $[Fe_4(OH)_4(PW_{10}O_{37})_2]^{10-}$, whereas the latter studied the sandwich anions $[Fe_4(H_2O)_2(PW_9O_{34})_2]^{6-}$ and $[Fe_4(H_2O)_2(P_2W_{15}O_{56})_2]^{12-}$. Structures of multi-iron polyoxotungstates (tungstosilicates, tungstogermanates and others) and of the anion $[Fe_4(H_2O)_2(FeW_9O_{34})_2]^{10-}$ were also reported.[34,35] The Fe–$O(H_2)$ bond lengths in the sandwich-type iron polyoxotungstophosphates were found to be around 2.00 Å.[33] Other values reported, for polyoxometalates or iron complexes, fall in the range 2.02–2.19 Å.[34,36] The average value reported for hexaaquairon(III) countercations in Keggin-type molybdophosphate compounds, obtained from EXAFS data, was 1.98 Å.[23] Thus, the Fe–O bond length corresponding to the oxygen from the terminal water molecule for the $PW_{11}Fe$ anion is possibly 1.943 Å in the solid sample and 1.976 Å in the $CH_3CN$ solution. With this assumption the average value of the equatorial Fe–O distances is 2.29 Å. The iron–oxygen distances found for the sandwich and the dimeric anions with P were in the range 1.88–1.99 Å for Fe–O–W and 2.18–2.40 Å in the Fe–O–P bridges.[32,33] In all cases the iron was octahedrally coordinated, but the arrangements of atoms around the $FeO_6$ octahedra in those anions are different from that of the monosubstituted $PW_{11}Fe$. The results obtained by EXAFS reported in this paper seem to indicate a larger and more distorted $FeO_6$ for $PW_{11}Fe$ than for the dimeric or the sandwich anions, which is obviously related to the difference in the structural arrangements, in which the possibility of an increase in Fe–O distances is higher for the less rigid $PW_{11}Fe$ anion. It is interesting to note that the Fe in $PW_{11}Fe$ is at a closer distance from the phosphorus heteroatom (3.105 Å in the solid, 3.156 Å in solution) than the W in the Keggin, lacunary, and iron-monosubstituted structures (3.545, 3.346, and 3.583, respectively, for solid samples). The enlargement of the $FeO_6$ octahedron is possibly accompanied by a rearrangement of the whole $FeW_2O_{13}$ group. Nevertheless, results from infrared spectroscopy suggest that there is not a significant distortion of the central $PO_4$ group.[37] The infrared spectrum, between 1000–1100 $cm^{-1}$, of the TBA salt of the $PW_{11}Fe$ anion has only one band,[38] assigned to the $\nu_{as}$(P–O) at 1069 $cm^{-1}$. The corresponding value for the $PW_{12}$ anion is 1080 $cm^{-1}$. The splitting of the $\nu_{as}$(P–O) is usually less pronounced for TBA than for K salts,[38] with the possible exception of the TBA salt of the $PW_{11}$ anion, for which the infrared spectrum shows two bands in this region at 1107 $cm^{-1}$ and 1054 $cm^{-1}$.[39]

### Mn *K* Edge Analysis of $[PW_{11}Mn(H_2O)O_{39}]^{4-}$

The Mn *K* edge analysis of $PW_{11}Mn$ indicated that there are six oxygen atoms in the first coordination sphere of Mn (Figure 5) with distances in the range of 1.981–2.626 Å (Table 6). The two W atoms in the same $W_2MnO_{13}$ group are at an average distance of 3.243 Å from Mn. The longest bond length was attributed to the Mn–O in the Mn–O–P group. This long Mn–O(–P) distance was considered to be evidence of Jahn–Teller tetragonal distortion of the octahedron around the high spin $Mn^{III}$ ion. One oxygen atom at 2.140 Å was attributed to the Mn–$O(H_2)$ group from a comparison with values reported by Zhang et al.[40] The average Mn–O bond lengths found in the EXAFS spectroscopic study described here are larger than the usual $Mn^{III}$–O bond lengths reported in the literature either in polyoxometalates[40,41] or otherwise.[42] As a consequence of the

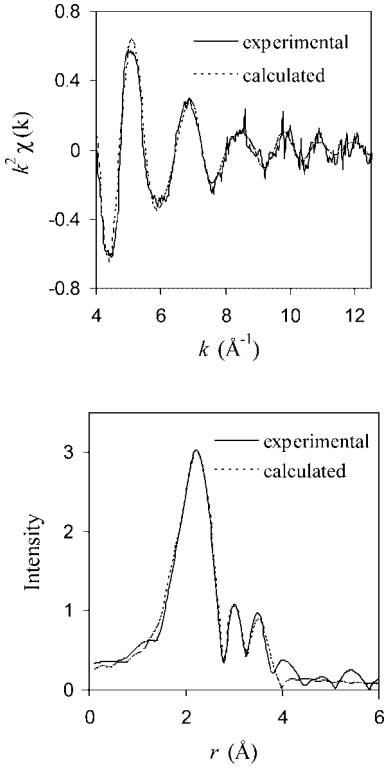


Figure 5. Mn *K* edge EXAFS spectrum and Fourier transform for $[PW_{11}Mn(H_2O)O_{39}]^{4-}$ in solid state TBA salt.

  

Jahn–Teller effect, the $Mn^{III}$ ion is possibly slightly out of the polyoxometalate vacancy of the $PW_{11}$ ligand, and this may be the reason for the long Mn–O bond length values found in this study. It may be noted, comparing the data in Table 4, Table 5, and Table 6, that the average of the M–O bond lengths in the $MO_6$ octahedra for M = Mn, Fe, (2.30 Å and 2.27 Å, respectively) are larger than the average W–O distances in $PW_{11}M$.

Table 6. EXAFS best-fit parameters for solid $TBA_4[PW_{11}Mn^{III}(H_2O)O_{39}]$ (Mn *K* edge fluorescence mode). Parameters as defined in Table 1.

| Shells | Solid state |
|---|---|
| R1 (1 × O) | 1.981 (0.007) |
| R2 (2 × O) | 2.140 (0.006) |
| R3 (2 × O) | 2.460 (0.008) |
| R4 (1 × O) | 2.626 (0.006) |
| R5 (2 × W) | 3.243 (0.016) |
| R7 (1 × P) | 3.128 (0.021) |
| *A*[1] | 0.020 (0.002) |
| *A*[2] | 0.012 (0.002) |
| *A*[3] | 0.007 (0.002) |
| *A*[4] | 0.010 (0.002) |
| *A*[5] | 0.028 (0.004) |
| *A*[7] | 0.024 (0.005) |
| $E_f$ (eV) | 8.2 |
| *R* (%) | 23.4 |

### $[PW_{11}Ru(H_2O)O_{39}]^{4-}$, Ru *K* Edge Analysis

Table 7 shows the distances from the shells to the Ru atom. The distance from the Ru atom to the first six oxygen atoms average 2.23 Å in the solid state (2.056–2.413 Å) and 2.35 Å in acetonitrile solution (2.106–2.603 Å). The two W atoms from the same $W_2RuO_{13}$ group ($W_1$ and $W_2$, Figure 1, a) are localized at 3.361 Å in the solid state and 3.410 Å in $CH_3CN$ solution (Table 7). Thus the structure of $PW_{11}Ru$ seems to be approximately the same in the solid compound and in solution. The phosphorus atom was found at a longer distance from ruthenium for the $PW_{11}Ru$ in acetonitrile than in the solid state (3.781 Å and 3.571 Å, respectively), and this is the only important difference when we compare these two environments (Table 7 and Figure 6).

Table 7. EXAFS best-fit parameters for $TBA_4[PW_{11}Ru^{III}(H_2O)O_{39}]\cdot H_2O$ (Ru *K* edge fluorescence mode). Parameters as defined in Table 1.

| Shells | Solid state | Shells | $CH_3CN$ solution |
|---|---|---|---|
| R2 (2 × O) | 2.056 (0.004) | R2 (2 × O) | 2.106 (0.004) |
| R3 (2 × O) | 2.234 (0.014) | R3 (2 × O) | 2.343 (0.010) |
| R4 (2 × O) | 2.413 (0.017) | R4 (2 × O) | 2.603 (0.010) |
| R5 (2 × W) | 3.361 (0.021) | R5 (2 × W) | 3.410(0.016) |
| R7 (1 × P) | 3.571 (0.049) | R7 (1 × P) | 3.781 (0.019) |
| R9 (2 × W) | 3.584 (0.046) | R9 (2 × W) | 3.564 (0.017) |
| *A*[2–3] | 0.010 (0.003) | *A*[2–3] | 0.020 (0.005) |
| *A*[4] | 0.003 (0.008) | *A*[4] | 0.014 (0.003) |
| *A*[7] | 0.009 (0.006) | *A*[7] | 0.023 (0.004) |
| *A*[5,9] | 0.020 (0.010) | *A*[5,9] | 0.008 (0.003) |
| $E_f$ (eV) | –4.8 | $E_f$ (eV) | –6.6 |
| *R* (%) | 26.5 | *R* (%) | 20.7 |

By comparing the EXAFS data of $PW_{11}Ru$ with $PW_{11}Fe$ it may be noted that the results suggested that the size of

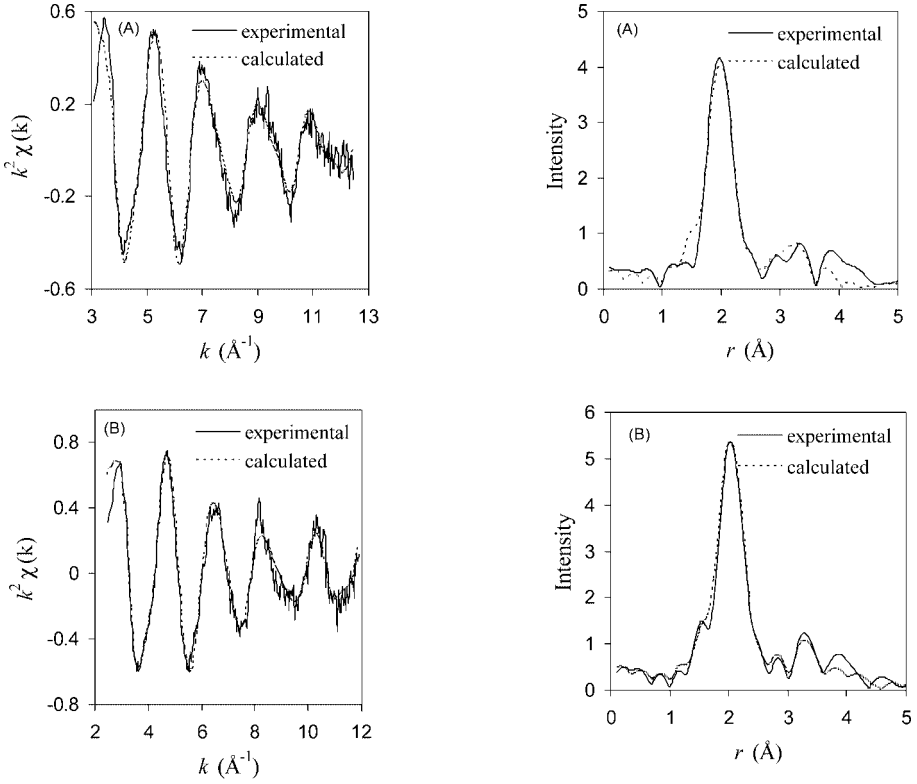


Figure 6. Ru *K* edge EXAFS spectrum and Fourier transform for $[PW_{11}Ru(H_2O)O_{39}]^{4-}$ in solid state TBA salt (a) and in $CH_3CN$ solution (b).

  

the $FeO_6$ and the $RuO_6$ octahedra were not very different. The Ru atom is at a longer distance from the heteroatom P than it is from Fe. Also, the size of the group $W_2RuO_{13}$ seems to be bigger than $W_2FeO_{13}$ because the distance from the Ru atom to the closest two W atoms, Ru–W, is larger than for Fe–W. The two other W atoms (outside the $W_2RuO_{13}$ unit) are at a distance from the Ru atom of 3.584 Å in the solid state and at 3.564 Å in the $CH_3CN$ solution.

The crystal structure of a salt of the anion $[SiW_{11}Ru^{III}(S\text{-}DMSO)O_{39}]^{5-}$ was reported recently.[43] This was the first Ru-monosubstituted Keggin ion in which the ruthenium center was not crystallographically disordered. The Ru–O bond lengths averaged 2.04 Å in this anion.[43];7

### Effect of Changing the Central Heteroatom X (P, Si, and B)

The effect of changing the central heteroatom (X) on the structure of polyoxotungstates was studied by comparing EXAFS data resulting from W $L_{III}$ edge analysis for $PW_{11}Mn^{III}$, $SiW_{11}Mn^{III}$, and $BW_{11}Mn^{III}$ (Figure 7 and Table 8). Because of the possible occurrence of the Jahn–Teller effect the environment of the Mn ion was expected to be more distorted than for other substituting metals. Thus, the ability of the $W_{11}Mn(H_2O)O_{39}$ unit to accommodate different heteroatom sizes of varying formal oxidation states could be studied in the solid compounds.

Table 8. EXAFS best-fit parameters for solid $TBA_4H[SiW_{11}Mn(H_2O)O_{39}]\cdot H_2O$ and $TBA_4H_2[BW_{11}Mn(H_2O)O_{39}]\cdot 2H_2O$ (W $L_{III}$ edge transmission mode). Parameters as defined in Table 1.

| Shells | $SiW_{11}Mn$ | Shells | $BW_{11}Mn$ |
|---|---|---|---|
| R1 (1 × O) | 1.717 (0.005) | R1 (1 × O) | 1.714 (0.007) |
| R2 (2 × O) | 1.883 (0.005) | R2 (2 × O) | 1.889 (0.006) |
| R3 (2 × O) | 2.010 (0.006) | R3 (2 × O) | 2.003 (0.008) |
| R4 (1 × O) | 2.277 (0.020) | R4 (1 × O) | 2.272 (0.012) |
| $R_{Mn}$ (1 × Mn) | 2.386 (0.024) | $R_{Mn}$ (1 × Mn) | 2.421 (0.016) |
| R5 (1 × W) | 3.388 (0.005) | R5 (1 × W) | 3.074 (0.019) |
| R9 (2 × W) | 3.744 (0.032) | R9 (2 × W) | 3.636 (0.009) |
| R10 (1 × Si) | 4.018 (0.030) | R10(1 × B) | 4.460 (0.057) |
| *A*[1] | 0.004 (0.001) | *A*[1] | 0.006 (0.001) |
| *A*[2–3] | 0.006 (0.001) | *A*[2–3] | 0.010 (0.002) |
| *A*[4] | 0.013 (0.004) | *A*[4] | 0.009 (0.003) |
| *A*[Mn] | 0.039 (0.005) | *A*[Mn] | 0.033 (0.003) |
| *A*[5,9] | 0.007 (0.004) | *A*[5,9] | 0.006 (0.004) |
| *A*[10] | 0.015 (0.008) | *A*[10] | 0.001 (0.002) |
| $E_f$ (eV) | 10.5 | $E_f$ (eV) | 10.8 |
| *R* (%) | 18.8 | *R* (%) | 20.1 |

The six oxygen atoms from the first coordination sphere $WO_6$ were localized in the range 1.717–2.277 Å for X = Si and 1.714–2.272 Å for X = B (Table 8). It can be noticed that the average W–$O_4$ distance (Figure 1, a) in the $WO_6$ octahedra are slightly smaller for the polyanion with X = P (Table 4). Contrary, the distance between the Mn atom and $W_c$ is bigger for X = P than for X = Si and B.

No relationship between the average bond lengths and the size of the central atom could be deduced (in line with published results for the parent Keggin anions[44,45]). Glob-

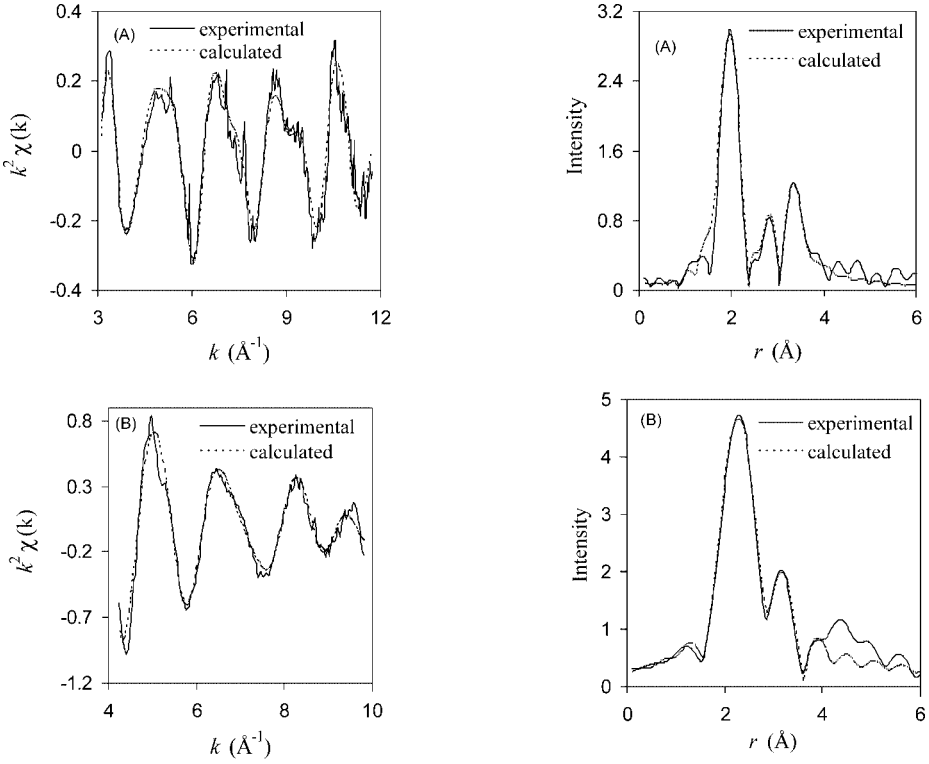


Figure 7. W $L_{III}$ edge EXAFS spectrum and Fourier transform for $[SiW_{11}Mn(H_2O)O_{39}]^{5-}$ (a) and $[BW_{11}Mn(H_2O)O_{39}]^{6-}$ (b) anions in solid state compounds.

  

ally, the size of the $W_3O_{13}$ groups seems to be independent of X because of the similarity between all X = P, Si, and B anions.

## Conclusions

EXAFS spectroscopy was used to characterize several tetrabutylammonium Keggin-type polyoxotungstates in the solid state and in acetonitrile solution. With this technique the local average environment around W and other substituting metals (Fe, Mn, Ru) was revealed in the lacunary and metal-substituted tungstophosphates $[PW_{11}O_{39}]^{7-}$ and $[PW_{11}M(H_2O)O_{39}]^{4-}$, M = Fe, Mn, Ru, and compared with that of the parent Keggin anion $[PW_{12}O_{40}]^{3-}$. These are compounds with interesting catalytic properties and the detailed knowledge of their structure, particularly around the lacunae or of the substituting metals, has unquestionable relevance. The average structure of W in the series $[XW_{11}Mn^{III}(H_2O)O_{39}]^{n-}$, X = P, Si, B was also obtained and compared. Of those anions, only the structure of $[PW_{12}O_{40}]^{3-}$ and $[PW_{11}O_{39}]^{7-}$ are known from crystallographic studies.[25,30] For the different anions EXAFS data allowed the determination of bond lengths and other interatomic distances in the vicinity of target atoms. The influence of the lacuna or of substituting metals on the W–O bond lengths was not, in general, very large, but could be noticed. The substituting metals (Fe, Mn, Ru) were coordinated by six oxygen atoms, but the coordination octahedron around Mn was found to be larger and more distorted than for the other metals. This was considered to be evidence of Jahn–Teller distortion.

For most cases little change in EXAFS and in the determined parameters occurred upon dissolution of the compounds in acetonitrile. The lacunary anion was, however, the most affected. EXAFS spectroscopy may be used to monitor the stability of the polyoxometalates in solution. The structure of the polyoxoanions in the presence of $H_2O_2$ will be described in a forthcoming paper. In this context, the results presented here may open a way of studying the fate of polyoxometalates in homogeneous catalysis in acetonitrile.

In conclusion, this EXAFS study allowed (1) the determination of structural information and details of metal coordination in these anions, not obtained to date by other techniques, in view of the natural difficulties introduced by the structural disorder, and (2) the comparison of the interatomic distances in different heteropolyanions of the same family in the solid state and in solution. This is the first systematic structural study using EXAFS of lacunary or metal-monosubstituted Keggin-type anions.

## Experimental Section

**Materials:** All reagents were used as received. Acetonitrile (Panreac, for instrumental analysis) and boron nitride (Aldrich) were used. The following compounds were prepared and purified as reported previously: $TBA_3[PW_{12}O_{40}]$,[46] $TBA_4H_3[PW_{11}O_{39}]$,[26] $TBA_4[PW_{11}M(H_2O)O_{39}]$, M = Fe[26] and Mn,[47] $TBA_4H[SiW_{11}Mn(H_2O)O_{39}]$,[47] and $TBA_4H_2[BW_{11}Mn(H_2O)O_{39}]\cdot H_2O$.[27] IR spectra of $PW_{11}Mn$ [$cm^{-1}$]: $\nu_{as}$(P–$O_a$) 1086, 1074 (s), $\nu_{as}$(W–$O_d$) 962 (vs), $\nu_{as}$(W–$O_b$–W) 881 (s), $\nu_{as}$(W–$O_c$–W), 804 (vs) ($O_d$, terminal oxygen, $O_b$, $O_c$, bridging oxygens, and $O_a$, central oxygen atom[46]). The general procedure used for the TBA salt of $PW_{11}Fe$[26] was adapted to prepare $TBA_4[PW_{11}Ru(H_2O)O_{39}]\cdot 4H_2O$:[48] aqueous solutions of $RuCl_3$ (Fluka) and $PW_{11}$, prepared in situ, were mixed at 90 °C; the solid obtained after the addition of aqueous TBABr was filtered and recrystallized in acetonitrile. Analytical data (%) with calculated values in parenthesis: C: 18.93 (20.03), H: 3.79 (4.05), N: 1.82 (1.46). The IR spectrum shows characteristic peaks attributed to $\nu_{as}$(W–$O_d$) at 945 $cm^{-1}$, $\nu_{as}$(W–$O_b$–W) at 892 $cm^{-1}$, $\nu_{as}$(W–$O_c$–W) at 820 $cm^{-1}$, and $\nu_{as}$(P–$O_a$) at 1080 and 1045 $cm^{-1}$.

**Data Collection and Analysis:** The extended X-ray absorption spectra associated with Fe (7.112 keV) or Mn (6.539 keV) *K* edges were collected in the fluorescence mode on stations 7.1 [double crystal Si (111) order-sorting monochromator] and with the Ru *K* edge (22.117 keV) on station 9.2 [double crystal Si (220) order-sorting monochromator]. W $L_{III}$ edge (10.207 keV) was collected in transmission mode on station 7.1. Both stations are located at Daresbury Laboratory (Synchrotron Radiation Source-SRS). The energy of the storage ring is 2 GeV and during the experiments the average current was 150 mA. Solid samples of polyoxotungstates were diluted when necessary with boron nitride and pressed into self supporting pellets with a typical thickness of 0.3 mm. Liquid samples of polyoxotungstates (10 mM) were prepared by direct dissolution of the compound in acetonitrile and placed in liquid cells that were 2 mm in thickness. The measurements were carried out at room temperature.

EXCALIB,[49] SPLINE,[50] and EXCURV98[51] were the programs used to process and analyze the EXAFS data. For each sample at least six scans were averaged. Curve-fitting analyses by least-squares refinement of the non-Fourier filtered $k^2$-weighted EXAFS data were carried out with the EXCURV98 program.[51] The calculations were performed using single scattering. The coordination number of each shell was fixed according to literature values. EXAFS refinements were performed in the *R* space. The number of parameters ($N_i$) was calculated for each refinement and this number indicates the number of parameters that can be refined. The number of shells that were fitted depended on the number of parameters determined. $N_i$ was quantified considering the distance range in the Fourier transform ($\Delta r$) and the energy range in EXAFS oscillations ($\Delta k$), $N_i = 2\Delta r\Delta k/\pi$. The number of parameters refined for each sample was smaller than $N_i$.

The analysis of the W $L_{III}$ edge structure of the Keggin anion $[PW_{12}O_{40}]^{3-}$ was done using as reference the published structural data.[25] For the lacunary $[PW_{11}O_{39}]^{7-}$ and for the substituted anions, $[XW_{11}M^{III}(H_2O)O_{39}]^{n-}$, X = P, M = Fe, Mn, Ru, and X = Si, B, M = Mn, this was done using the X-ray single crystal data of the similar lacunary anion $[SiW_{11}O_{39}]^{8-}$,[31] and of the $[PW_{11}Co(H_2O)O_{39}]^{5-}$ polyanion,[11] respectively.

## Acknowledgments

Thanks go to Daresbury Laboratory (synchrotron Radiation source-SRS) for the EXAFS analysis and to Fundação para Ciência e Tecnologia (FCT) and the University of Aveiro for the financial support of this work. M. S. B. is grateful to FCT and FEDER for her PhD grant.

  

[1] M. T. Pope, *Heteropoly and Isopoly Oxometalates*, Springer-Verlag, Berlin, **1983**.

[2] M. T. Pope, A. Muller, *Angew. Chem. Int. Ed. Engl.* **1991**, *30*, 34–48.

[3] M. T. Pope, A. Muller (Eds.), *Polyoxometalate Chemistry: From Topology via Self-assembly Applications*, Kluwer, Dordrecht, **2001**.

[4] M. T. Pope, A. Muller (Eds.), *Polyoxometalates: From Platonic Solids to Antirectroviral Activity*, Kluwer, Dordrecht, **1994**.

[5] a) R. Neumann in *Modern Oxidative Methods* (Ed.: J. E. Bäckvall), Wiley-VCH, Weinheim, **2004**, ch. 8; b) R. Neumann, *Prog. Inorg. Chem.* **1998**, *47*, 317–370; c) I. V. Kozhevnikov, *Chem. Rev.* **1998**, *98*, 171–198; d) C. L. Hill, C. M. Prosser-McCartha, *Coord. Chem. Rev.* **1995**, *143*, 407–455.

[6] a) T. Okuhara, N. Mizuno, M. Misono, *Appl. Catal. A* **2001**, *222*, 63–77; b) N. Mizuno, M. Misono, *Chem. Rev.* **1998**, *98*, 199–217.

[7] a) E. Coronado, P. Day, *Chem. Rev.* **2004**, *104*, 5419–5448; b) P. Gomez-Romero, *Adv. Mater.* **2001**, *13*, 163–174; c) J. M. Clemente-Juan, E. Coronado, *Coord. Chem. Rev.* **1999**, *193–195*, 361–394; d) E. Coronado, C. J. Gomez-Garcia, *Chem. Rev.* **1998**, *98*, 273–296; e) L. Ouahab, *Coord. Chem. Rev.* **1998**, *178–180*, 1501–1531.

[8] J. T. Rhule, C. L. Hill, D. A. Judd, *Chem. Rev.* **1998**, *98*, 327–357.

[9] A. M. V. Cavaleiro, J. D. Pedrosa de Jesus, H. I. S. Nogueira in *Metal Clusters in Chemistry* (Eds.: P. Braunstein, L. A. Oro, P. R. Raithby), Wiley-VCH, Weinheim, **1999**, vol. 1, p. 444–458.

[10] a) J. F. Keggin, *Proc. R. Soc.* **1934**, *A144*, 75–100; b) J. F. Keggin, *Nature* **1933**, *131*, 908–909.

[11] H. T. Evans, T. J. R. Weakley, G. B. Jameson, *J. Chem. Soc., Dalton Trans.* **1996**, 2537–2540.

[12] J. R. Galan-Mascaros, C. Gimenez-Saiz, S. Triki, C. J. Gomez-Garcia, E. Coronado, L. Ouahab, *Angew. Chem. Int. Ed. Engl.* **1995**, *34*, 1460–1462.

[13] E. Coronado, J. R. Galan-Mascaros, C. Gimenez-Saiz, C. J. Gomez-Garcia, S. Triki, *J. Am. Chem. Soc.* **1998**, *120*, 4671–4681.

[14] B. Yan, Y. Xu, X. Bu, N. K. Goh, L. S. Chia, G. D. Stucky, *J. Chem. Soc., Dalton Trans.* **2001**, 2009–2014.

[15] Z. Han, Y. Zhao, J. Peng, H. Ma, Q. Liu, E. Wang, *J. Mol. Stuct.* **2005**, *738*, 1–7.

[16] J. Niu, Z. Wang, J. Wang, *J. Solid State Chem.* **2004**, *177*, 3411–3417.

[17] J. Evans, M. Pillinger, J. M. Rummey, *J. Chem. Soc., Dalton Trans.* **1996**, 2951–2961.

[18] T. Miyanaga, T. Fujikawa, N. Matubayashi, T. Fukumoto, K. Yokoi, I. Watanabe, S. Ikeda, *Bull. Chem. Soc. Jpn.* **1989**, *62*, 1791–1796.

[19] X. Zhang, M. T. Pope, M. R. Chance, G. B. Jameson, *Polyhedron* **1995**, *14*, 1381–1392.

[20] G. Muncaster, G. Sankar, C. R. A. Catlow, J. M. Thomas, S. J. Coles, M. Hursthouse, *Chem. Mater.* **2000**, *12*, 16–18.

[21] a) A. D. Newman, D. R. Brown, P. Siril, A. F. Lee, K. Wilson, *Phys. Chem. Chem. Phys.* **2006**, *8*, 2893–2902; b) B. B. Bardin, R. J. Davis, *App. Catal. A* **2000**, *200*, 219–231; c) D. E. Clinton, D. A. Tryk, I. T. Bae, F. L. Urbach, M. R. Antonio, D. A. Scherson, *J. Phys. Chem.* **1996**, *100*, 18511–18514.

[22] a) T. Ressler, O. Timpe, F. Girgsdies, J. Wienold, T. Neisius, *J. Catal.* **2005**, *231*, 279–291; b) T. Ressler, O. Timpe, F. Girgsdies, *Z. Kristallogr.* **2005**, *220*, 295–305; c) M. H. Tran, H. Ohkita, T. Mizushima, N. Kakuta, *Appl. Catal. A: General* **2005**, *287*, 129–134; d) C. J. Dillon, J. H. Holles, R. J. Davis, J. A. Labinger, M. E. Davis, *J. Catal.* **2003**, *218*, 54–66; e) J. Wienold, O. Timpe, T. Ressler, *Chem. Eur. J.* **2003**, *9*, 6007–6017; f) F. C. Jentoft, S. Klokishner, J. Krohnert, J. Melsheimer, T. Ressler, O. Timpe, J. Wienold, R. Schlogl, *App. Catal. A* **2003**, *256*, 291–317; g) T. Sugino, A. Kido, N. Azuma, A. Ueno, Y. Udagawa, *J. Catal.* **2000**, *190*, 118–127; h) B. B. Bardin, R. J. Davis, *App. Catal. A* **1999**, *185*, 283–292.

[23] Q. Huynh, J. M. M. Millet, *J. Phys. Chem. Solids* **2005**, *66*, 887–894.

[24] a) H. Carabineiro, R. Villaneau, X. Carrier, P. Herson, F. Lemos, F. R. Ribeiro, A. Proust, M. Che, *Inorg. Chem.* **2006**, *45*, 1915–1923; b) C. Martin, C. Lamonier, M. Fournier, O. Mentré, V. Harlé, D. Guillaume, E. Payen, *Chem. Mater.* **2005**, *17*, 4438–4448 and references cited therein; c) M. Chiang, M. R. Antonio, C. W. Williams, L. Soderholm, *Dalton Trans.* **2004**, 801–806 and references cited therein; d) R. Villaneau, H. Carabineiro, X. Carrier, R. Thouvenot, P. Herson, F. Lemos, F. R. Ribeiro, M. Che, *J. Phys. Chem. B* **2004**, *108*, 12465–12471; e) R. Villaneau, A. Proust, F. Robert, F. Villain, M. Verdaguer, P. Gouzerth, *Polyhedron* **2003**, *22*, 1157–1165 and references cited therein; f) I. Pettiti, I. L. Botto, C. I. Cabello, S. Colonna, M. Faticanti, G. Minelli, P. Porta, H. J. Thomas, *Appl. Catal A: General* **2001**, *220*, 113–121.

[25] G. M. Brown, M. R. Noe-Spirlet, W. R. Busing, H. A. Levy, *Acta Crystallogr., Sect. B* **1977**, *33*, 1038–1046.

[26] M. M. Q. Simões, C. M. M. Conceição, J. A. F. Gamelas, P. M. D. N. Domingues, A. M. V. Cavaleiro, J. A. S. Cavaleiro, A. J. V. Ferrer-Correia, R. A. W. Johnstone, *J. Mol. Catal. A* **1999**, *144*, 461–468.

[27] I. C. M. S. Santos, M. M. Q. Simões, S. M. M. M. Pereira, R. R. L. Martins, M. G. P. M. S. Neves, J. A. S. Cavaleiro, A. M. V. Cavaleiro, *J. Mol. Catal. A* **2003**, *195*, 253–262.

[28] a) M. M. Q. Simões, I. C. M. S. Santos, M. S. S. Balula, J. A. F. Gamelas, A. M. V. Cavaleiro, M. G. P. M. S. Neves, J. A. S. Cavaleiro, *Catal. Today* **2004**, *91–92*, 211–214; b) M. S. S. Balula, I. C. M. S. Santos, M. M. Q. Simões, M. G. P. M. S. Neves, J. A. S. Cavaleiro, A. M. V. Cavaleiro, *J. Mol. Catal. A* **2004**, *222*, 159–165; c) I. M. S. Santos, M. S. S. Balula, M. M. Q. Simões, M. G. P. M. S. Neves, J. A. S. Cavaleiro, A. M. V. Cavaleiro, *Synlett* **2003**, 1643–1646.

[29] N. Binsted, D. Norman, *Jpn. J. Appl. Phys. 1* **1993**, *32*, 342–346, Suppl. 32–2.

[30] J. Fuchs, A. Thiele, R. Palm, *Z. Naturforsch., Teil B* **1981**, *36*, 544–550.

[31] K. Y. Matsumoto, Y. Sasaki, *Bull. Chem. Soc. Jpn.* **1976**, *49*, 156–158.

[32] M. Li, S. Jin, H. Liu, G. Xie, M. Chen, Z. Xu, X. You, *Polyhedron* **1998**, *17*, 3721–3725.

[33] a) X. Zhang, Q. Chen, D. C. Duncan, C. F. Campana, C. L. Hill, *Inorg. Chem.* **1997**, *36*, 4208–4215; b) X. Zhang, Q. Chen, D. C. Duncan, R. J. Lachicotte, C. L. Hill, *Inorg. Chem.* **1997**, *36*, 4381–4386.

[34] a) B. Botar, Y. V. Geletii, P. Kogerler, D. G. Musaev, K. Morokuma, I. A. Weinstock, C. L. Hill, *J. Am. Chem. Soc.* **2006**, *128*, 11268–11277; b) T. M. Anderson, W. A. Neiwert, K. I. Hardcastle, C. L. Hill, *Inorg. Chem.* **2004**, *43*, 7353–7358; c) E. M. Limanski, M. Piepenbrink, E. Droste, K. Burgemeister, B. Krebs, *J. Cluster Sci.* **2002**, *13*, 369–378; d) I. Loose, E. Droste, M. Bosing, H. Pohlmann, M. H. Dickman, C. Rosu, M. T. Pope, B. Krebs, *Inorg. Chem.* **1999**, *38*, 2688–2694.

[35] a) L. Bi, U. Kortz, S. Nellutla, A. C. Stowe, J. Tol, N. S. Dalal, B. Keita, L. Nadjo, *Inorg. Chem.* **2005**, *44*, 896–903; b) S. H. Wasfi, A. L. Reingold, G. F. Kokoszka, A. S. Golstein, *Inorg. Chem.* **1987**, *26*, 2934–2939.

[36] a) S. Poussereau, G. Blondin, G. Chottard, J. Guilhem, L. Tchertanov, E. Riviere, J. J. Girerd, *Eur. J. Inorg. Chem.* **2001**, 1057–1062; b) P. C. Junk, B. J. McCool, B. Moubaraki, K. S. Murray, L. Spiccia, *Angew. Chem. Int. Ed.* **1999**, *38*, 2224–2226.

[37] C. Rocchiccioli-Deltcheff, R. Thouvenot, *J. Chem. Res. (S)* **1977**, 46–47.

[38] J. A. F. Gamelas, F. A. Couto, M. C. Trovão, A. M. V. Cavaleiro, J. A. S. Cavaleiro, J. D. Pedrosa de Jesus, *Thermochim. Acta* **1999**, *326*, 165–173.

[39] E. Radkov, R. H. Beer, *Polyhedron* **1995**, *14*, 2139–2143.


  

[40] a) X. Zhang, C. J. O'Connor, G. B. Jameson, M. T. Pope, *Inorg. Chem.* **1996**, *35*, 30–34; b) X. Zhang, G. B. Jameson, C. J. O'Connor, M. T. Pope, *Polyhedron* **1996**, *15*, 917–922.
[41] D. Drewes, M. Piepenbrink, B. Krebs, *J. Clust. Sci.* **2006**, *17*, 361–374.
[42] B. Chiswell, E. D. McKenzie in *Comprehensive Coordination Chemistry* (Eds.: G. Wilkinson, R. D. Gillard, J. A. McCleverty), Pergamon Press, Oxford, **1987**, vol. 4, p. 1.
[43] M. Sadakane, D. Tsukuma, M. H. Dickman, B. Bassil, U. Kortz, M. Higashijima, W. Ueda, *Dalton Trans.* **2006**, 4271–4276.
[44] A. L. Nolan, C. C. Allen, R. C. Burns, D. C. Craig, G. A. Lawrance, *Aust. J. Chem.* **2000**, *53*, 59–66.
[45] H. Fletcher, C. C. Allen, R. C. Burns, D. C. Craig, *Acta Crystallogr., Sect. C* **2001**, *57*, 505–507.
[46] C. Rocchiccioli-Deltcheff, M. Fournier, R. Franck, R. Thouvenot, *Inorg. Chem.* **1983**, *22*, 207–216.
[47] M. S. Balula, J. A. Gamelas, H. M. Carapuça, A. M. V. Cavaleiro, W. Schlindwein, *Eur. J. Inorg. Chem.* **2004**, 619–628.
[48] C. Rong, M. T. Pope, *J. Am. Chem. Soc.* **1992**, *114*, 2932–2938.
[49] *EXCALIB*, CCLRC Daresbury Laboratory Computer Program, **1982**.
[50] *Exspline*, a program for EXAFS background subtraction, Daresbury Laboratory, **2000**, based on an original program, P. Ellis Spline, PhD Thesis, University of Sydney, **1995**.
[51] N. Binsted, *EXCURV98*, CCLRC Daresbury Laboratory computer program, **1998**.

Received: July 28, 2005
Extented Version Received: November 28, 2006
Published Online: February 2, 2007

  